Inorganic Chemistry

Article

pubs.acs.org/IC

Stereochemical Diversity of {MNO}^{10} Complexes: Molecular Orbital Analyses of Nickel and Copper Nitrosyls

Jeanet Conradie[†,‡] and Abhik Ghosh*[,†]

[†]Department of Chemistry and Center for Theoretical and Computational Chemistry, University of Tromsø, N-9037 Tromsø, Norway

[‡]Department of Chemistry, University of the Free State, 9300 Bloemfontein, Republic of South Africa

Supporting Information

ABSTRACT: The great majority of {NiNO}^{10} complexes are characterized by short Ni−N(O) distances of 1.60−1.65 Å and linear NO units. Against this backdrop, the {CuNO}^{10} unit in the recently reported $[Cu(CH_3NO_2)_5(NO)]^{2+}$ cation (**1**) has a CuNO angle of about 120° and a very long 1.96 Å Cu−N(O) bond. According to DFT calculations, metal−NO bonding in **1** consists of a single Cu(d_{z^2})−NO(π^*) σ-interaction and essentially no metal(d_π)−NO(π^*) π-bonding, which explains both the bent CuNO geometry and the long, weak Cu−N(O) bond. This σ-interaction is strongly favored by a ligand *trans* to the NO; indeed such a *trans* ligand may be critical for the existence and stability of a {CuNO}^{10} unit. By contrast, {NiNO}^{10} complexes exhibit a strong avoidance of such *trans* ligands. Thus, a five-coordinate {NiNO}^{10} complex appears to favor a trigonal-bipyramidal structure with the NO in an equatorial position, as in the case of $[Ni(bipy)_2(NO)]^+$ (**6**). An unusual set of Ni(d)−NO(π^*) orbital interactions accounts for the strongly bent NiNO geometry for this complex.

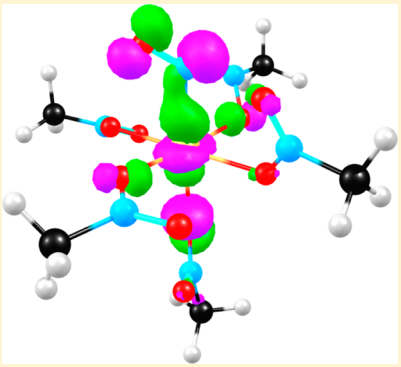

1. INTRODUCTION

The mechanism of copper nitrite reductase (CuNIR), which reduces nitrite to NO, has been suggested to involve a {CuNO}^{10} intermediate.[1,2] Such intermediates have also been infrequently postulated in synthetic model studies,[3] but only very recently have the first such species been fully characterized.[4] The crystal structure of the {CuNO}^{10} complex $[Cu(CH_3NO_2)_5(NO)](PF_6)_2$, recently reported by Hayton and co-workers,[4] reveals a strongly bent CuNO angle of about 121° as well as a long Cu−N(O) distance of about 1.96 Å (Figure 1). To put these metrical parameters in perspective, we may note that numerous {NiNO}^{10} complexes are known, the vast majority of which feature essentially linear nitrosyl groups (Figure 2);[5−10] several {CuNO}^{11} complexes are also known, and these are characterized Cu−N(O) distances of only about 1.76−1.79 Å.[11] Complicating the picture, however, are a small handful of {NiNO}^{10} complexes in which the NiNO angle is strongly bent, that is, <140°. Thus, Caulton and co-workers reported a four-coordinate {NiNO}^{10}−PNP complex with a strongly bent NiNO group.[12] Similarly, $[Ni(bipy)_2(NO)]^+$ and another similar complex, also reported by the Hayton group, contain strongly bent NiNO units.[13] The unusual structures of $[Cu(CH_3NO_2)_5(NO)]^{2+}$, Caulton's {NiNO}^{10}−PNP complex, and $[Ni(bipy)_2(NO)]^+$ cannot be ascribed to crystal packing forces but clearly point to a more elemental origin, which can only be one or more unusual aspects of the metal−NO bonding.[14] In this study, we have sought to clarify the nature of this bonding in terms of a simple molecular orbital picture, which emerged relatively straightforwardly from a set of density functional theory (DFT) calculations, as described below.

2. METHODS

The DFT calculations were generally carried out with the BP86[15,16] functional and the Gaussian09[17] program system. A few calculations were also cross-checked with the B3LYP[18] functional, with no significant discrepancies. We employed the 6-311G(d,p) basis set for first-row atoms, McLean−Chandler (12s, 9p) → (621111, 52111)[19] basis sets for second-row atoms, and all-electron Wachters−Hay[20] basis sets for first-row transition elements. Fine meshes for numerical integration of matrix elements and suitably tight criteria for SCF and geometry optimization were used throughout.

3. MOLECULAR STRUCTURES

We have noted for some time the generally excellent performance of DFT with respect to metal−nitrosyl structures, and that is also the case in this study.[14c] The significance of an accurate optimized structure is that it is a strong indication that the underlying electronic-structural description is correct. Gratifyingly, our calculations reproduced the salient structural features of the various {MNO}^{10} complexes examined, including $[Cu(CH_3NO_2)_5(NO)]^{2+}$ (**1**), three relatively typical linear {NiNO}^{10} complexes **2**−**4**, Caulton's {NiNO}^{10}−PNP complex (**5**), and $[Ni(bipy)_2(NO)]^+$ (**6**).

As shown in Figure 1, the long Cu−N(O) distance and the strongly bent CuNO angle of **1** are well reproduced by both BP86 and B3LYP calculations.[4] The optimized geometries also do a fair job of capturing the subtle variations in Cu−O distances that are observed in the crystallographic structure of

Received: November 17, 2013
Published: May 5, 2014

   dx.doi.org/10.1021/ic4028157 | *Inorg. Chem.* 2014, 53, 4847−4855

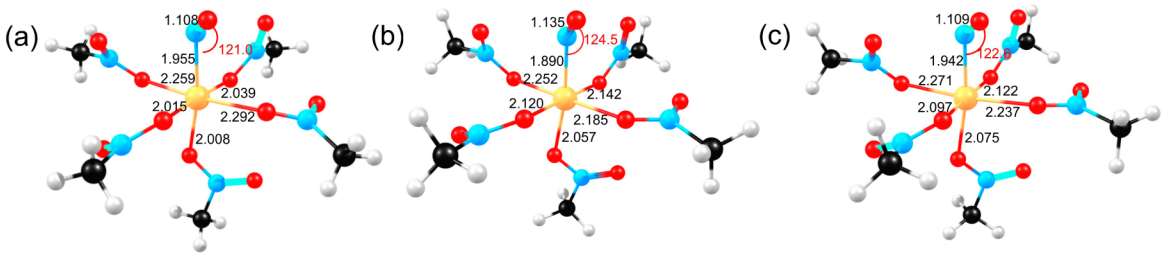

Figure 1. (a) Experimental, (b) BP86, and (c) B3LYP (C_1) geometries (Å, deg) of $[Cu(CH_3NO_2)_5(NO)]^{2+}$ (**1**). Color code: C black, N blue, O red, H pearl, and Cu light orange.

1. If we define the Cu−N vector as the approximate *z* direction, the four shortest Cu−N/O bonds may then be thought of as lying in the *yz* plane; the two Cu−O bonds along the *x* axis are then roughly 0.2 Å longer than the other Cu−O bonds.

Experimentally, complex **1** exhibits an unusually high NO stretching frequency (ν_{NO}) of 1933 cm^{-1},[4] which is higher by over 200 cm^{-1} than that of the {CuNO}[11] complex $Tp^{tBu}Cu(NO)$ (1712 cm^{-1}).[11] Vibrational analyses (BP86) were carried on both complexes, yielding unscaled ν_{NO}'s of 1917.7 and 1717.0 cm^{-1}, in excellent agreement with experimental results, which may be viewed as an additional check on the quality of the calculations reported herein.

Figure 2 shows that BP86 calculations also reproduce the observed linear NiNO units with short Ni−N(O) distances of 1.60−1.65 Å for complexes **2**−**4**, as well as the bent NiNO units of **5** and **6**. The geometry of complex **6** may be described as roughly trigonal bipyramidal with the NO occupying an equatorial position.

4. MOLECULAR ORBITAL DESCRIPTION OF METAL−NO BONDING IN COMPLEX 1

To appreciate the essentials of the Cu-NO bonding in **1**, it is useful to simplify the problem by symmetrizing the complex to C_s. Thus, Figure 3 presents the main d-based valence MOs of **1**, for both a C_s-constrained but otherwise fully optimized geometry and an artificial C_s geometry where the CuNO angle has been constrained to near-linearity.[21] A striking feature of **1** is that the MOs do not evince any trace of Cu(d_π)−NO(π^*) π-bonding. The Cu−N(O) bond thus consists of a single Cu(d_{z^2})−NO(π^*) σ-interaction, which explains both the length and the observed weakness of the bond; the topology of this orbital (similar to the analogous orbital in {FeNO}[7] and {CoNO}[8] porphyrins[14,22]) also explains the strongly bent geometry of the {CuNO}[10] unit.[23]

We are now in a position to consider the subtle variations in Cu−O distances that have been observed for complex **1**. As mentioned above, a symmetry-unconstrained DFT geometry optimization (Figure 1) successfully captures these variations. Figure 4 shows that the highest occupied d_{z^2}-based MO of **1** (obtained from a symmetry-unconstrained optimization) is not quite cylindrically symmetric about the Cu−N(O) axis but rather engages in antibonding interactions with two oppositely placed oxygens in the equatorial plane but not with the other two oxygens. Stated differently, this "d_{z^2}" orbital also has significant $d_{x^2-z^2}$ character. The lower symmetry of this hybrid "d_{z^2}" orbital provides an explanation for the diversity of Cu−O distances observed for complex **1**, which may be viewed as a pseudo-Jahn−Teller distortion. The effect evidently arises from the near-degeneracy of the d_{z^2}- and $d_{x^2-y^2}$-based MOs. The complex may break symmetry in the equatorial *xy* plane by stretching along either the *x* or the *y* axis, suggesting that, in solution, **1** should exhibit a fluxional structure.

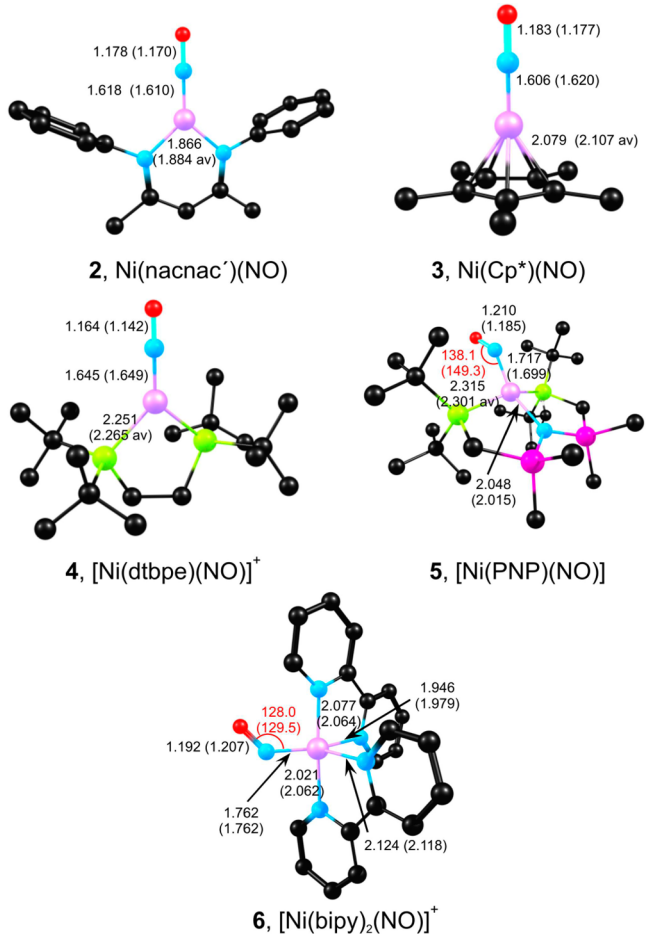

Figure 2. Calculated BP86 and experimental (in parentheses, averaged where applicable) bond lengths (Å) of selected {NiNO}[10] complexes. Color code for atoms: C black, N blue, O red, P lime green, Si magenta, and Ni lilac. Hydrogens have been omitted for clarity.

5. MOLECULAR ORBITAL CONSIDERATIONS FOR NI−NO BONDING IN COMPLEXES 2−5

The {NiNO}[10] complexes Ni(nacnac′)(NO) (**2**),[5] Ni(Cp*)-(NO) (**3**),[10] and $[Ni(dtbpe)(NO)]^+$ [**4**, dtbpe = 1,2-bis(di-*t*-butylphosphino)ethane],[6] which may be viewed as paradigms of {MNO}[10] complexes, provide an appropriate backdrop against which we can appreciate the unique geometric and electronic structure of **1**. Figure 4 provides a visual comparison of the highest occupied d_{z^2}-based MO of **1** with that of complexes **2**−**4**. Observe that for **2**−**4**, this MO also has

dx.doi.org/10.1021/ic4028157 | Inorg. Chem. 2014, 53, 4847−4855

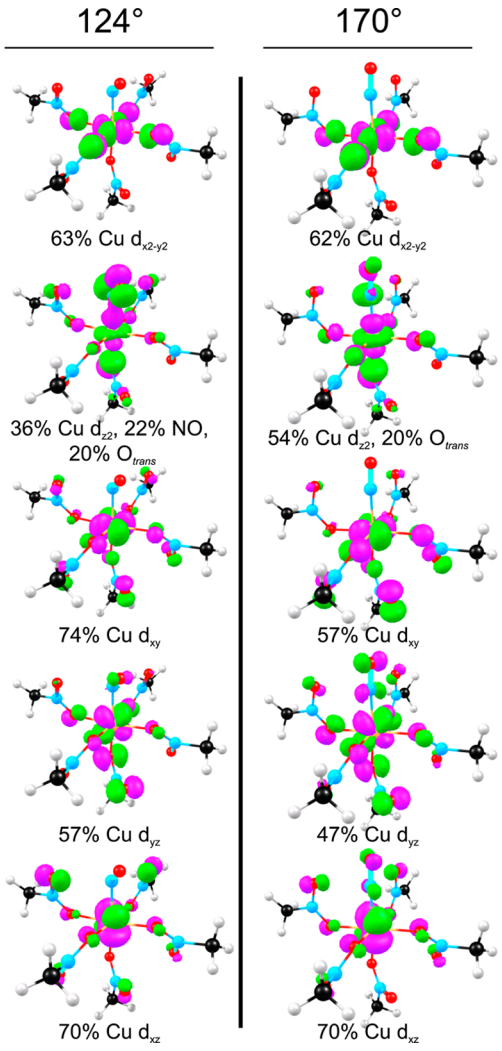

Figure 3. BP86 d-based MOs for two C_s symmetry-constrained geometries of **1**. Contour = 0.06 e/Å^3.

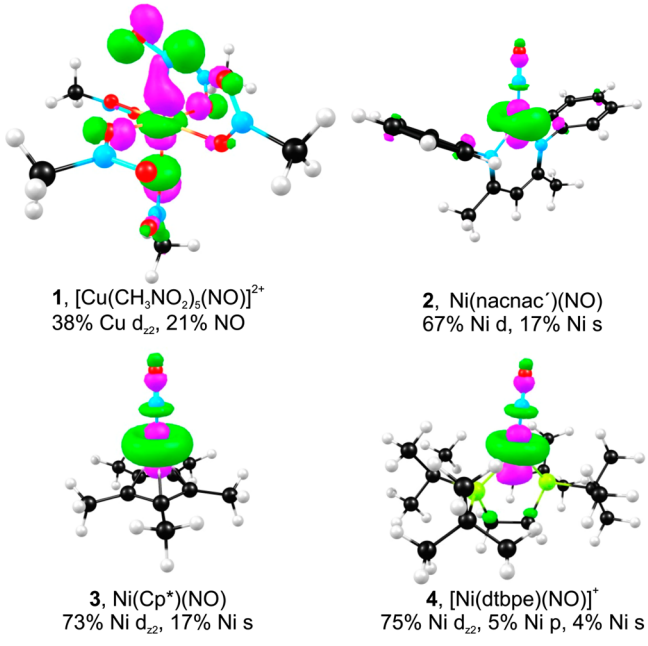

Figure 4. Comparison of BP86 d_{z^2}-based MOs of **1**–**4**.

significant Ni s or p character or both. Such s/p infusion has also been invoked to rationalize the linearity of certain {FeNO}^{7} units,[24] including those in $[Fe(CN)_4(NO)]^{2-}$ (S = 1/2)[24a] and $[Fe(S^tBu)_3(NO)]^-$ (S = 3/2).[24b] The effect of such mixing is a relatively shrunken "top" lobe of the d_{z^2} orbital, which engages in only a weak antibonding interaction with the nitrogen lone pair on the NO, resulting in a linear metal–NO geometry. As shown in Figure 4, such s/p infusion typically also results in an enlarged "central lobe" (e.g., complexes **2** and **3**) or an enlarged "bottom lobe" (e.g., complex **4**) of the d_{z^2}-based orbital.[25] These orbital hybridizations are clearly facilitated by the lack of ligands that are strictly equatorial with respect to the NO in complexes **2**–**4** and by the lack of *trans* ligands in **3** and **4**.

Walsh diagrams (Figure 5) and metal–NO bending potentials (Figure 6) help place the above insights on a firmer footing.[26] Thus, the d_{z^2}-based MO of **1** is strongly destabilized as the CuNO unit is linearized, providing a clear explanation for **1**'s strongly bent CuNO unit. By contrast, the d-based MOs of **2** are modestly affected by the NiNO angle; only the Ni(d_π)–NO(π^*) π-bonding MOs are mildly destabilized by bending of the NiNO angle. As a result, the MNO bending potential of **1** is characterized by a sharp, relatively steep-walled minimum, whereas **2**, as well as heme–NO complexes, exhibit rather more flat-bottomed bending potentials (Figure 6).[14,27]

We may now apply these ideas to complex **5**, whose geometry may be described as either distorted square-planar or flattened-tetrahedral. For a pincer-like, tridentate PNP supporting ligand, a square-planar complex might have been a reasonable prediction. The presence of a strong anionic nitrogen ligand *trans* to the NO, however, would strongly destabilize the d_σ-based MO that would be responsible for metal–NO σ-bonding, as well as prevent any infusion of metal s/p character into that MO. A bent NO, coupled with modest tetrahedralization, is expected to lessen the impact of this antibonding interaction,[2] thereby providing a qualitative explanation for the unique geometry of **5**. The five primarily d-based HOMOs of **5** are depicted in Figure 7: observe that none of these MOs involves a particularly prohibitive antibonding interaction involving the anionic nitrogen (N_{ax}) *trans* to the NO.

6. MOLECULAR ORBITAL DESCRIPTION OF COMPLEX 6

Figure 8 depicts the five HOMOs of $[Ni(bipy)_2(NO)]^+$ (**6**), which, conveniently for our discussion, also correspond to the five highest occupied d-based MOs. If we align the Ni–N(O) bond along the z axis, the HOMO may be described as a Ni(d_{y^2}) orbital with lobes pointing toward the pyridines along the trigonal axis of the trigonal bipyramid. The central annular lobe of this orbital engages in a key σ-interaction with one of the NO π^* MOs. Except for d_{xy} orbital, which is δ-like with respect to the Ni–N(O) vector, all the other d orbitals also engage in significant bonding interactions with an NO π^* MO. Had the NO been linear, two of the Ni(d)–NO(π^*) bonding interactions, involving the d_{y^2} and the $d_{x^2-z^2}$ orbitals, would not be possible on symmetry grounds, which is essentially the rationale for the bent NO group in complex **6**.

Figure 9 presents Walsh diagram analyses and potential energy scans that shed further light on the above reasoning. Widening the NiNO angle while optimizing all other internal coordinates (Figure 9a) led to significant stabilization of three of the five primarily d-based occupied MOs, thus revealing no

dx.doi.org/10.1021/ic4028157 | Inorg. Chem. 2014, 53, 4847–4855

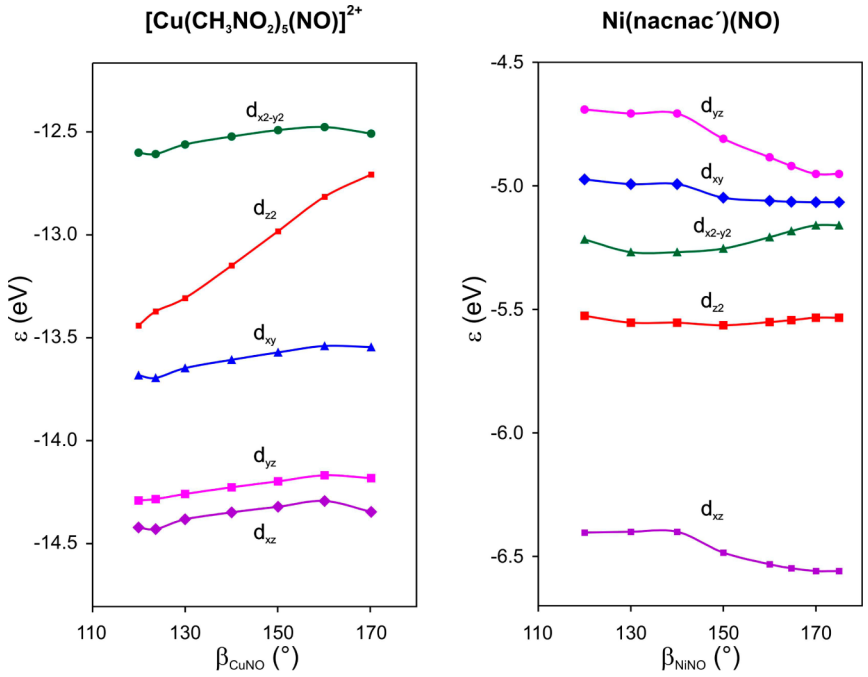

Figure 5. BP86 Walsh diagrams for the d-MOs of **1** (left) and **2** (right).[25]

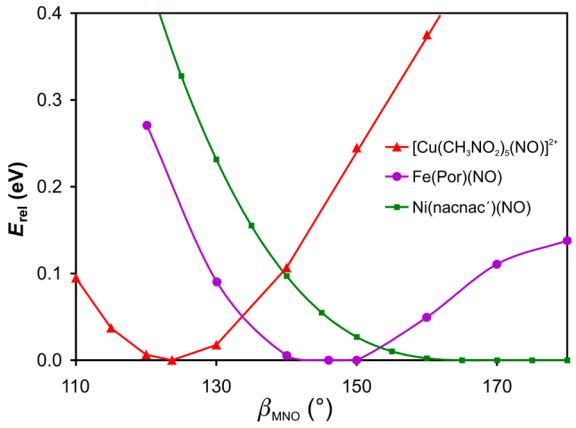

Figure 6. BP86 MNO bending potentials for **1**, **2**, and Fe(Por)(NO).[26]

MO-based impetus for a strongly bent NiNO group. An examination of the molecular total energy as a function of the widening NiNO angle (Figure 9c) also exibited a modest increase in energy on the order of a few kilocalories per mole. Careful examination of the optimized structures showed that, as the NiNO angle is widened beyond about 140°, one of the Ni–N(bipy) bonds gradually breaks up. To preclude such bond breakage, we carried out a second Walsh analysis (Figure 9b), where we constrained the Ni(bipy)$_2$ unit at the same geometry as that in the optimized structure of complex **6**. Under these conditions, the d_{y^2} orbital exhibited a steep rise in energy as the NiNO bond was linearized, consistent with disruption of the σ-interaction involving the central annular lobe mentioned above. The overall conclusion thus appears to be that, for a five-coordinate {NiNO}^{10} complex with relatively weak-field to moderately strong-field ligands, a trigonal-bipyramidal geometry with the NO as an equatorial ligand affords maximum metal–ligand bonding.

7. FIVE-COORDINATE {CUNO}^{10} COMPLEXES

Optimization of [Cu(bipy)$_2$(NO)]$^{2+}$ (**7**), the hypothetical {CuNO}^{10} analogue of **6**, yielded a different structure relative to **6**. Both complexes are approximately trigonal bipyramidal, but as shown in Figure 10, **7** has the NO as an axial ligand, *trans* with respect to one of the pyridines. As in the case of **1**, the BP86 geometry [Cu(bipy)$_2$(NO)]$^{2+}$ exhibits a long Cu–N(O) bond of 1.925 Å. As for **1**, the d-based HOMOs show no indication of Cu(d_π)–NO(π^*) π-bonding. A single, relatively weak Cu($d_{x^2-z^2}$)–NO(π^*) σ-interaction, shown in Figure 10, essentially accounts for the entire Cu–NO bonding. This MO also shows an antibonding interaction involving a *trans* pyridine ligand, which should enhance the Lewis basicity of the otherwise poorly basic Cu($d_{x^2-z^2}$) electrons. Indeed, this "push effect" may be so critical that a *trans* ligand may be a structural requirement for a moderately stable {CuNO}^{10} unit. A BP86 vibrational analysis on **7** predicts a ν_{NO} of 1844.6 cm^{-1}, not unlike but lower than that obtained for **1**, consistent with a somewhat stronger push effect in **7** relative to **1**.

Our hypothesis is clearly satisfied for the octahedral complex **1**. Five-coordinate {CuNO}^{10} complexes, where a ligand *trans* with respect to the NO can potentially be avoided, may provide a more stringent test of our hypothesis. Unfortunately, no five-coordinate {CuNO}^{10} crystal structures have been reported. Mondal and co-workers, however, have claimed to have generated the five-coordinate complex [CuL$_2$(NO)]$^{2+}$ (**8**, L = 2-(2-aminoethyl)pyridine) in solution.[3] DFT calculations by these authors indicated a square-pyramidal structure for **8** with the NO in an equatorial position. We have reexamined **8** in this study and found three different but essentially equienergetic minima, which are shown in Figure 11. The three stereoisomers include two trigonal-bipyramidal structures, TBP$_{ax1}$ and TBP$_{ax2}$ in Figure 11, both with the NO along the trigonal axis, and the square-pyramidal form with an equatorial NO, SQPy$_{eq}$, which was reported by Mondal and co-workers. Like complex **1**, all three isomers are characterized by a long Cu–N(O) bond (1.96 ± 0.01 Å) and a strongly bent CuNO angle (122° ± 2°).

dx.doi.org/10.1021/ic4028157 | Inorg. Chem. 2014, 53, 4847–4855

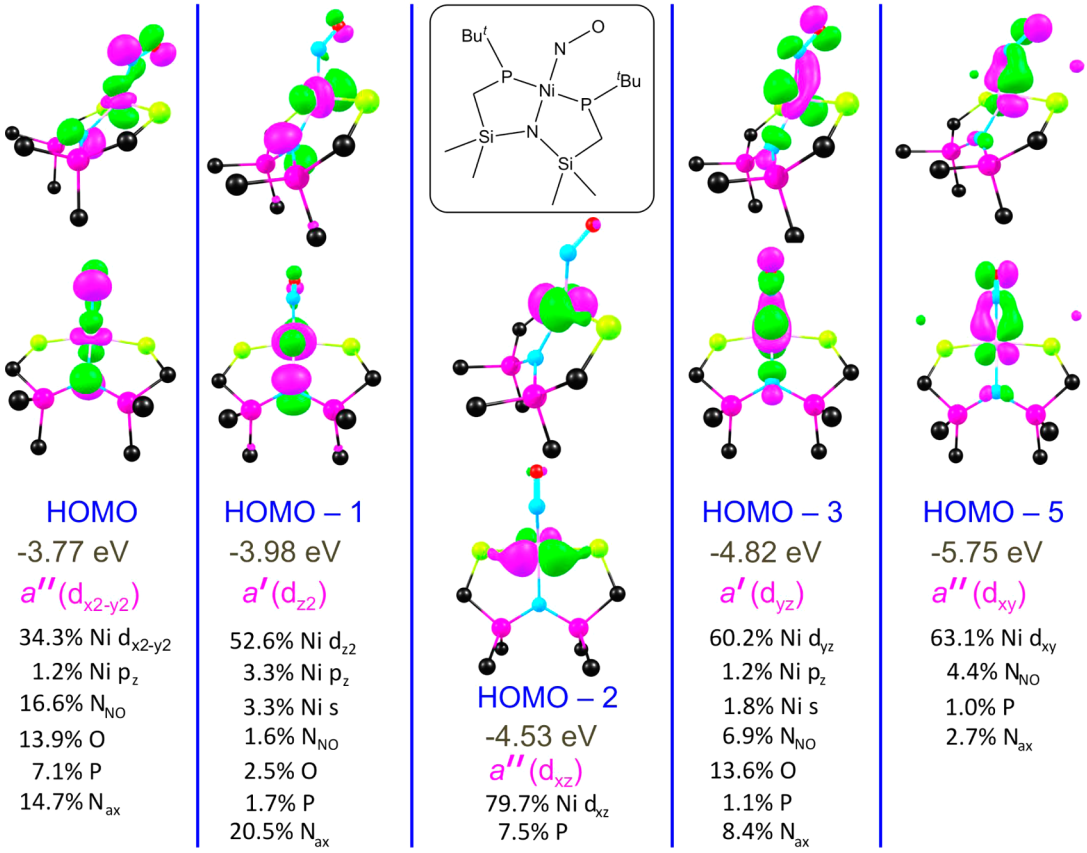

Figure 7. The primarily d-based HOMOs of complex **5** (C_s).

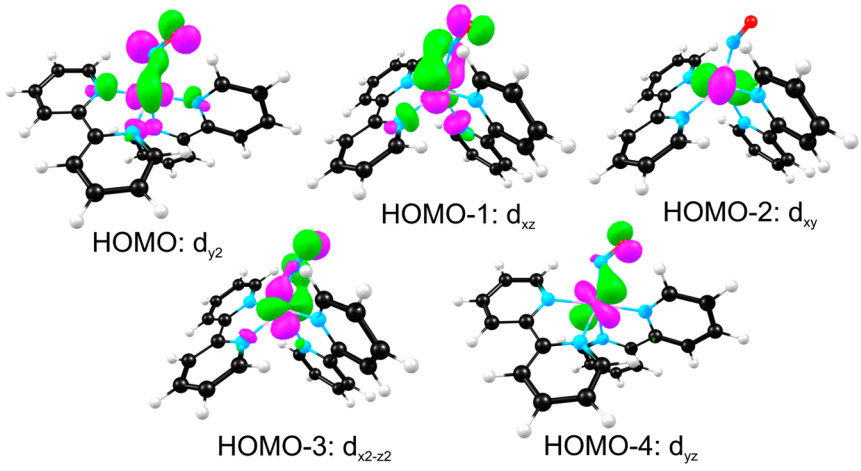

Figure 8. The Ni d-based HOMOs of complex **6**.

The NO in all three isomers also has a *trans* amine/pyridine ligand, consistent with our hypothesis. Conspicuously absent is a fourth potential isomer where the NO would be an equatorial ligand in a trigonal bipyramid and thus not have a *trans* ligand.

Vibrational analyses (BP86) of the three potential energy minima of **8** yielded ν_{NO}'s of 1820.9 (TBP_{ax1}), 1794.8 (TBP_{ax2}), and 1813.2 cm^{-1} ($SQPy_{eq}$), which are some 150−200 cm^{-1} higher than that experimentally measured for **8** (1630 cm^{-1}).[3] In our opinion, such high errors are implausible for the computational methods used in this study, which suggests that the structure of **8** may have been incorrectly assigned in the literature. One possibility is that **8** is a copper(I) nitrite complex, which would also be consistent with the fact that it is EPR-silent.

To further test our hypothesis, we also explored part of the potential energy surface of the hypothetical five-coordinate $\{CuNO\}^{10}$ complex $[Cu(CH_3NO_2)_4(NO)]^{2+}$ (**9**). Two different minima were found, indicated in Figure 12 as TBP_{ax} and $SQPy_{eq}$; both are characterized by the presence of a nitromethane ligand *trans* to the NO. No square-pyramidal minimum with an axial NO could be located as a minimum-energy structure. To estimate the energy of such a structure, we optimized **9** while constraining the four equatorial, coordinated oxygens to a single plane and freezing the equatorial Cu−O

dx.doi.org/10.1021/ic4028157 | Inorg. Chem. 2014, 53, 4847−4855

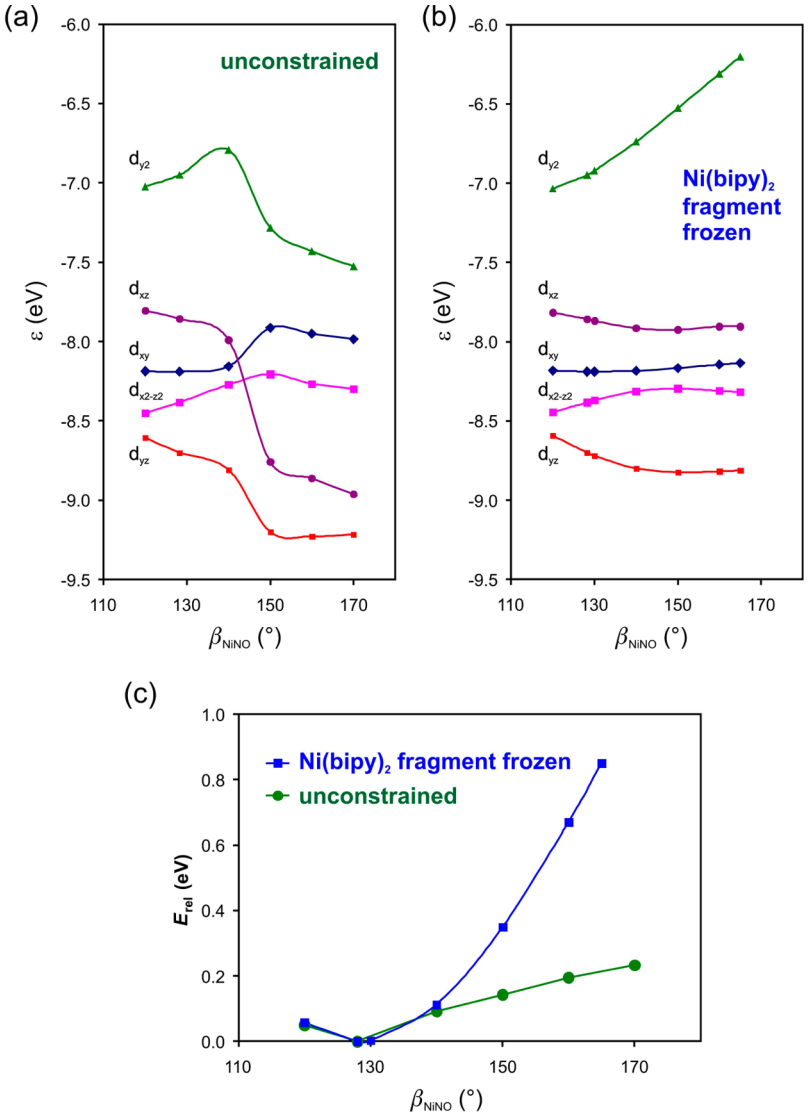

Figure 9. Walsh diagrams for highest occupied d-based MOs of **6** as a function of the NiNO angle (a) with all other internal coordinates fully optimized and (b) with the $Ni(bipy)_2$ fragment frozen at the equilibrium geometry for **6**. (c) Potential energy scans as a function of the NiNO angle for the two different deformation pathways.

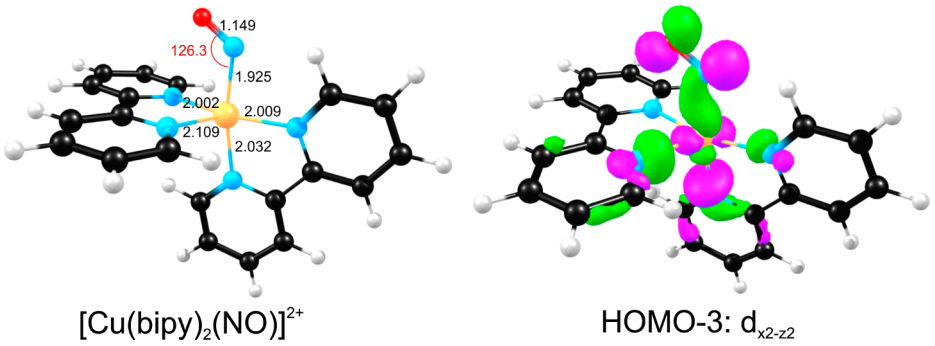

Figure 10. Key aspects of the optimized geometry (Å, deg) and a plot of the $Cu(d_{x^2-z^2})$–$NO(\pi^*)$ σ-interaction for $[Cu(bipy)_2(NO)]^{2+}$ (**7**). The atomic composition for this MO is 28% Cu $d_{x^2-z^2}$, 12% N_{NO}, 13% O, 13% N_{ax}.

distances at the same values as those in complex **1**. The energy of such an artificially constrained structure, indicated as $SQPy_{ax}$* in Figure 12, turned out to be 0.33 eV above the global minimum. Overall, therefore, we believe that a *trans* ligand is an essential structural requirement for a moderately stable $\{CuNO\}^{10}$ complex.

dx.doi.org/10.1021/ic4028157 | *Inorg. Chem.* 2014, 53, 4847−4855

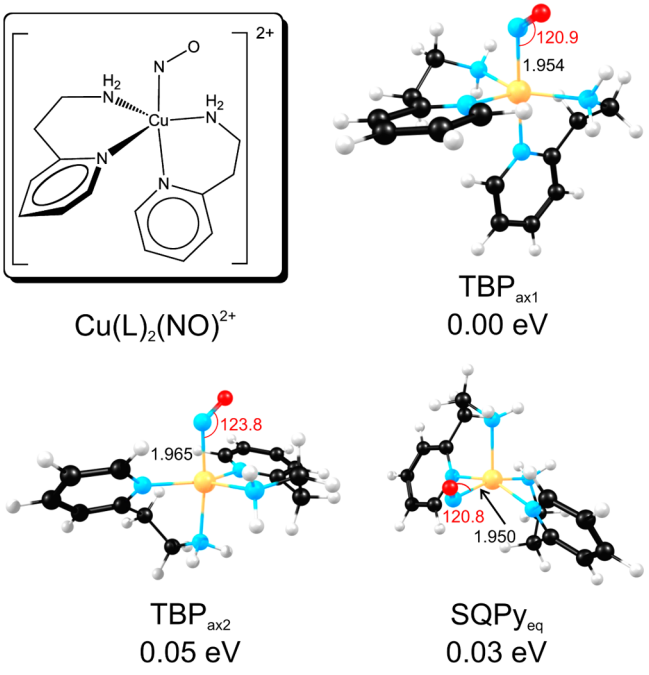

Figure 11. BP86 minima for $[Cu(L)_2(NO)]^{2+}$ (**8**), where L = 2-(2-aminoethyl)pyridine. Color code for atoms: Cu orange, C black, N cyan, O red, and H pearl. Relative energies (eV), Cu–N(O) distances (Å, black), and CuNO angles (deg, red) are also shown.

8. CONCLUDING REMARKS

Pseudotetrahedral and trigonal-planar $\{NiNO\}^{10}$ complexes may justifiably viewed as the paradigm of $\{MNO\}^{10}$ complexes. These complexes are characterized by a short Ni–N(O) distance of 1.60–1.65 Å and essentially linear NiNO units. A handful of complexes stand out against this structural paradigm, prompting us to seek a deeper understanding of the factors affecting the stereochemistry of $\{MNO\}^{10}$ complexes. DFT calculations have now provided a broad, molecular-orbital-based explanation of this stereochemical diversity, the key points being as follows.

(a) The short Ni–N(O) distance and an essentially linear NiNO angle of a typical $\{NiNO\}^{10}$ unit reflect the optimum geometry for $Ni(d_\pi)$–$NO(\pi^*)$ π-bonding and, almost equally importantly, the lack of a *trans* ligand that could induce NO bending.

(b) A $\{CuNO\}^{10}$ unit, unlike a $\{NiNO\}^{10}$ unit, is not low-valent, and there is little imperative for $Cu(d_\pi)$–$NO(\pi^*)$ π-bonding. Metal–NO bonding in a $\{CuNO\}^{10}$ complex accordingly consists of a single $Cu(d_\sigma)$–$NO(\pi^*)$ σ-interaction, which explains both the length and weakness of the Cu–N(O) linkage as well as the strongly bent shape of the CuNO group, as observed for the cationic complex $[Cu(CH_3NO_2)_5(NO)]^{2+}$ (**1**).

(c) When forced to have a *trans* ligand, as in complex **5**, an $\{NiNO\}^{10}$ unit undergoes strong bending.

(d) Five-coordination is rare for $\{NiNO\}^{10}$ complexes, but when it does occur (e.g., complex **6**), a trigonal-bipyramidal geometry is preferred, with the NO in the equatorial position. A remarkable set of orbital interactions results in a strongly bent NiNO group in such a complex.

(e) The low-valent $\{NiNO\}^{10}$ group avoids having not only a *trans* ligand but also ligands equatorial with respect to the Ni–N(O) vector. In doing so, the $Ni(d_\sigma)$ orbitals avoid strong antibonding interactions with ligand lone pairs. These stereochemical imperatives are reflected in the broad prevalence of trigonal-planar and pseudotetrahedral coordination geometries. By contrast, a *trans* ligand appears to be a structural *requirement* for the existence and stability of a $\{CuNO\}^{10}$ group.

■ ASSOCIATED CONTENT

Ⓢ Supporting Information

Optimized Cartesian coordinates of the various molecules studied. This material is available free of charge via the Internet at http://pubs.acs.org.

■ AUTHOR INFORMATION

Corresponding Author

*E-mail: abhik@chem.uit.no.

Notes

The authors declare no competing financial interest.

■ ACKNOWLEDGMENTS

This work was supported by the Research Council of Norway and National Research Foundation of the Republic of South Africa.

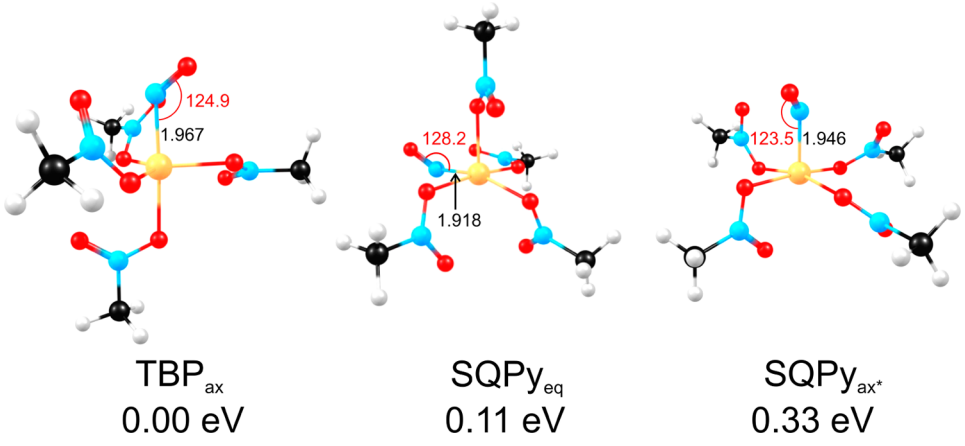

Figure 12. BP86 optimized structures for $[Cu(CH_3NO_2)_4(NO)]^{2+}$ (**9**).

dx.doi.org/10.1021/ic4028157 | *Inorg. Chem.* 2014, 53, 4847–4855

REFERENCES

(1) (a) Averill, B. A. *Chem. Rev.* **1996**, *96*, 2951−2964. (b) Wasser, I. M.; de Vries, S.; Moenne-Loccoz, P.; Schroder, I.; Karlin, K. D. *Chem. Rev.* **2002**, *102*, 1201−1234.

(2) The superscript 10 refers to the Enemark−Felham electron count, defined as the total number of metal d and NO π^* electrons: Enemark, J. H.; Feltham, R. D. *Coord. Chem. Rev.* **1974**, *13*, 339−406.

(3) Sarma, M.; Mondal, B. *Inorg. Chem.* **2011**, *50*, 3206−3212.

(4) Wright, A. M.; Wu, G.; Hayton, T. W. *J. Am. Chem. Soc.* **2010**, *132*, 14336−14337.

(5) Mononuclear trigonal-planar: Puiu, S. C.; Warren, T. H. *Organometallics* **2003**, *22*, 3974−3976 The simplified nacnac′ ligand used in our calculations has unsubstituted phenyl groups on the coordinating nitrogens..

(6) Mononuclear trigonal-planar: (a) Iluc, V. M.; Miller, A. J. M.; Hillhouse, G. L. *Chem. Commun.* **2005**, 5091−5093. (b) Varonka, M. S.; Warren, T. H. *Organometallics* **2010**, *29*, 717−720.

(7) Bi- and polynuclear trigonal-planar: Chong, K. S.; Rettig, S. J.; Storr, A.; Trotter, J. *Can. J. Chem.* **1979**, *57*, 3090−3098.

(8) Mononuclear pseudotetrahedral: (a) Meiners, J. H.; Rix, C. J.; Clardy, J. C.; Verkade, J. G. *Inorg. Chem.* **1975**, *14*, 705−710. (b) Haller, K. J.; Enemark, J. H. *Inorg. Chem.* **1978**, *17*, 3552−3558. (c) Fanariotis, I. A.; Christidis, P. C.; Rentzeperis, P. J. *Z. Kristallogr.* **1983**, *164*, 109−119. (d) Elbaze, G.; Dahan, F.; Dartiguenave, M.; Dartiguenave, Y. *Inorg. Chim. Acta* **1984**, *87*, 91−97. (e) Rahman, A. F. M. M.; Salem, G.; Stephens, F. S.; Wild, S. B. *Inorg. Chem.* **1990**, *29*, 5225−5230. (f) Darensbourg, D. J.; Decuir, T. J.; Stafford, N. W.; Robertson, J. B.; Draper, J. D.; Reibenspies, J. H.; Katho, A.; Joo, F. *Inorg. Chem.* **1997**, *36*, 4218−4226. (g) Schebler, P. J.; Riordan, C. G.; Guzei, I. A.; Rheingold, A. L. *Inorg. Chem.* **1998**, *37*, 4754−4755. (h) Liaw, W.-F.; Chiang, C.-Y.; Lee, G.-H.; Peng, S.-M.; Lai, C.-H.; Darensbourg, M. Y. *Inorg. Chem.* **2000**, *39*, 480−484. (i) MacBeth, C. E.; Thomas, J. C.; Betley, T. A.; Peters, J. C. *Inorg. Chem.* **2004**, *43*, 4645−4662. (j) Maffett, L. S.; Gunter, K. L.; Kreisel, K. A.; Yap, G. P. A.; Rabinovich, D. *Polyhedron* **2007**, *26*, 4758−4764. (k) Landry, V. K.; Pang, K.; Quan, S. M.; Parkin, G. *Dalton Trans.* **2007**, 820−824. (l) Landry, V. K.; Parkin, G. *Polyhedron* **2007**, *26*, 4751−4757. (m) Tennyson, A. G.; Dhar, A.; Lippard, S. J. *J. Am. Chem. Soc.* **2008**, *130*, 15087−15098. (n) Nieto, I.; Bontchev, R. P.; Ozarowski, A.; Smirov, D.; Krzystek, J.; Telser, J.; Smith, J. M. *Inorg. Chim. Acta* **2009**, *362*, 4449−4460. (o) Wright, A. M.; Wu, G.; Hayton, T. W. *Inorg. Chem.* **2011**, *50*, 11746−11753. (p) Munoz, S. B., III; Foster, W. K.; Lin, H.-J.; Margarit, C. G.; Dickie, D. A.; Smith, J. M. *Inorg. Chem.* **2012**, *51*, 12660−12668.

(9) Bi- and polynuclear pseudotetrahedral: (a) Chong, K. S.; Rettig, S. J.; Storr, A.; Trotter, J. *Can. J. Chem.* **1979**, *57*, 3107−3112. (b) Kriege-Simondsen, J.; Feltham, R. D. *Inorg. Chim. Acta* **1983**, *71*, 185−194. (c) Rauchfuss, T. B.; Gammon, S. D.; Weatherill, T. D.; Wilson, S. R. *New J. Chem.* **1988**, *12*, 373. (d) Haller, K. J.; Enemark, J. H. *Inorg. Chem.* **1978**, *17*, 3552−3558. (e) Del Zotto, A.; Mezzetti, A.; Novelli, V.; Rigo, P.; Lanfranchi, M.; Tiripicchio, A. *J. Chem. Soc., Dalton Trans.* **1990**, 1035−1042. (f) Vicic, D. A.; Anderson, T. J.; Cowan, J. A.; Schultz, A. J. *J. Am. Chem. Soc.* **2004**, *126*, 8132−8133.

(10) With Cp and arene ligands: (a) Fomitchev, D. V.; Furlani, T. R.; Coppens, P. *Inorg. Chem.* **1998**, *37*, 1519−1526. (b) Heinemann, F. W.; Pritzkow, H.; Zeller, M.; Zenneck, U. *Organometallics* **2000**, *19*, 4283−4288. See also ref 8o.

(11) (a) Ruggiero, C. E.; Carrier, S. M.; Antholine, W. E.; Whittaker, J. W.; Cramer, C. J.; Tolman, W. B. *J. Am. Chem. Soc.* **1993**, *115*, 11285−12298. (b) Carrier, S. M.; Ruggiero, C. E.; Tolman, W. B.; Jameson, G. B. *J. Am. Chem. Soc.* **1992**, *114*, 4407−4408. (c) Merkle, A. C.; Lehnert, N. *Inorg. Chem.* **2009**, *48*, 11504−11506.

(12) Fullmer, B. C.; Pink, M.; Fan, H.; Yang, X.; Baik, M.-H.; Caulton, K. G. *Inorg. Chem.* **2008**, *47*, 3888−3892.

(13) Wright, A. M.; Wu, G.; Hayton, T. W. *J. Am. Chem. Soc.* **2012**, *134*, 9930−9933.

(14) (a) Westcott, B. L.; Enemark, J. H. In *Inorganic Electronic Structure and Spectroscopy*; Solomon, E. I., Lever, A. B. P., Eds.; Wiley: New York, 1999; Vol. 2, pp 403−450 and refereneces therein. (b) Ghosh, A.; Hopmann, K. H.; Conradie, J. In *Computational Inorganic and Bioinorganic Chemistry*; Solomon, E. I., Scott, R. A., King, R. B., Eds.; John Wiley & Sons, Ltd: Chichester, U.K., 2009; pp 389−410. (c) Ghosh, A. *Acc. Chem. Res.* **2005**, *38*, 943−954.

(15) (a) Becke, A. D. *Phys. Rev.* **1988**, *A38*, 3098−3100. (b) Perdew, J. P. *Phys. Rev.* **1986**, *B33*, 8822. Erratum: Perdew, J. P. *Phys. Rev.* **1986**, *B34*, 7406.

(16) The choice of a pure (nonhybrid) functional was dictated by our desire to avoid broken-symmetry wavefunctions, which would have led to an unnecessarily complicated picture of the bonding. See, for example, Conradie, J.; Ghosh, A. *J. Phys. Chem. B* **2007**, *111*, 12621−12624.

(17) Frisch, M. J.; Trucks, G. W.; Schlegel, H. B.; Scuseria, G. E.; Robb, M. A.; Cheeseman, J. R.; Scalmani, G.; Barone, V.; Mennucci, B.; Petersson, G. A.; Nakatsuji, H.; Caricato, M.; Li, X.; Hratchian, H. P.; Izmaylov, A. F.; Bloino, J.; Zheng, G.; Sonnenberg, J. L.; Hada, M.; Ehara, M.; Toyota, K.; Fukuda, R.; Hasegawa, J.; Ishida, M.; Nakajima, T.; Honda, Y.; Kitao, O.; Nakai, H.; Vreven, T.; Montgomery, J. A., Jr.; Peralta, J. E.; Ogliaro, F.; Bearpark, M.; Heyd, J. J.; Brothers, E.; Kudin, K. N.; Staroverov, V. N.; Kobayashi, R.; Normand, J.; Raghavachari, K.; Rendell, A.; Burant, J. C.; Iyengar, S. S.; Tomasi, J.; Cossi, M.; Rega, N.; Millam, J. M.; Klene, M.; Knox, J. E.; Cross, J. B.; Bakken, V.; Adamo, C.; Jaramillo, J.; Gomperts, R.; Stratmann, R. E.; Yazyev, O.; Austin, A. J.; Cammi, R.; Pomelli, C.; Ochterski, J. W.; Martin, R. L.; Morokuma, K.; Zakrzewski, V. G.; Voth, G. A.; Salvador, P.; Dannenberg, J. J.; Dapprich, S.; Daniels, A. D.; Farkas, O.; Foresman, J. B.; Ortiz, J. V.; Cioslowski, J.; Fox, D. J. *Gaussian 09*, revision B.01; Gaussian, Inc.: Wallingford, CT, 2009.

(18) (a) Lee, C.; Yang, W.; Parr, R. G. *Phys. Rev. B* **1988**, *37*, 785−789. (b) Becke, A. D. *Phys. Rev. A* **1988**, *38*, 3098−3100. (c) Becke, A. D. *J. Chem. Phys.* **1992**, *96*, 2155−2160. (d) Becke, A. D. *J. Chem. Phys.* **1992**, *97*, 9173−9177. (e) Becke, A. D. *J. Chem. Phys.* **1993**, *98*, 5648−5652.

(19) (a) McLean, A. D.; Chandler, G. S. *J. Chem. Phys.* **1980**, *72*, 5639−5648. (b) Raghavachari, K.; Binkley, J. S.; Seeger, R.; Pople, J. A. *J. Chem. Phys.* **1980**, *72*, 650−654.

(20) (a) Wachters, A. J. H. *J. Chem. Phys.* **1970**, *52*, 1033−1036. (b) Hay, P. J. *J. Chem. Phys.* **1977**, *66*, 4377−4384.

(21) We will see that a C_s symmetry constraint is not entirely justified; it was however adopted here to facilitate a Walsh diagram analysis for uncovering the broad features of the electronic structure.

(22) For a survey of metalloporphyrin−NO_x structures, see: Wyllie, G. R. A.; Scheidt, W. R. *Chem. Rev.* **2002**, *102*, 1067−1090.

(23) Many NO researchers like to describe metal-bound nitrosyls as NO^+, $NO^\bullet$, or NO^-. According to the MO coefficients, the electrons in the Cu−NO σ-bond in **1** are roughly evenly shared between the Cu and the NO. This supports the Cu^{II}−$NO^\bullet$ description proposed by Hayton and co-workers.[4] In our opinion, however, such an antiferromagnetically coupled description is not particularly meaningful in the absence of a corresponding ferromagnetically coupled, bound state (which does not exist, according to our calculations). Under these circumstances, a covalent MO description appears to be preferable.

(24) (a) Conradie, J.; Ghosh, A. *J. Inorg. Biochem.* **2006**, *100*, 2069−2073. (b) Conradie, J.; Quarless, D. A., Jr.; Hsu, H.-F.; Harrop, T. C.; Lippard, S. J.; Koch, S. A.; Ghosh, A. *J. Am. Chem. Soc.* **2007**, *129*, 10446−10456. (c) Conradie, J.; Hopmann, J.; Ghosh, A. *J. Phys. Chem. B* **2010**, *114*, 8517−8524. (d) Conradie, J.; Ghosh, A. *Inorg. Chem.* **2011**, *50*, 4223−4225. (e) Patra, A. K.; Dube, K. S.; Conradie, J.; Ghosh, A.; Harrop, T. C. *Chem. Sci.* **2012**, *3*, 364−369.

(25) Ni(Cp*)(NO) may be viewed as a special case in this regard; although the Cp* ligand as a whole is *trans* to the NO, there is no specific atom located *trans* to the NO. The same holds true for the recently reported cationic complex $[Ni(mesitylene)(NO)]^+$, which also has a linear NO group.[8o]

(26) For simplicity, these calculations were carried out under a C_s symmetry constraint. For **2**, the NiNO angle was bent perpendicular to the plane of the β-diketiminato group.

(27) Thus, modest deviations of the NiNO group from strict linearity are not unexpected. A tristhiolate-supported $\{NiNO\}^{10}$ complex, reported by Lippard and co-workers, exhibits modest bending of the NiNO group.[8m]

dx.doi.org/10.1021/ic4028157 | *Inorg. Chem.* 2014, 53, 4847−4855